Clinical Cancer Research

Cancer-Stimulated CAFs Enhance Monocyte Differentiation and Protumoral TAM Activation via IL6 and GM-CSF Secretion

Haaglim Cho[1], Youngha Seo[1], Kin Man Loke[1], Seon-Wook Kim[1], Seong-Min Oh[1], Jun-Hyeong Kim[1], Jihee Soh[2], Hyoen Sik Kim[3], Hyunju Lee[2], Jin Kim[4], Jung-Joon Min[3], Da-Woon Jung[1], and Darren Reece Williams[1]

Abstract

Purpose: M2-type TAMs are increasingly implicated as a crucial factor promoting metastasis. Numerous cell types dictate monocyte differentiation into M2 TAMs via a complex network of cytokine-based communication. Elucidating critical pathways in this network can provide new targets for inhibiting metastasis. In this study, we focused on cancer cells, CAFs, and monocytes as a major node in this network.

Experimental Design: Monocyte cocultures with cancer-stimulated CAFs were used to investigate differentiation into M2-like TAMs. Cytokine array analyses were employed to discover the CAF-derived regulators of differentiation. These regulators were validated in primary CAFs and bone marrow-derived monocytes. Orthotopic, syngeneic colon carcinoma models using cotransplanted CAFs were established to observe effects on tumor growth and metastasis. To confirm a correlation with clinical evidence, meta-analyses were employed using the Oncomine database.

Results: Our coculture studies identify IL6 and GM-CSF as the pivotal signals released from cancer cell–activated CAFs that cooperate to induce monocyte differentiation into M2-like TAMs. In orthotopic, syngeneic colon carcinoma mouse models, cotransplanted CAFs elevated IL6 and GM-CSF levels, TAM infiltration, and metastasis. These pathologic effects were dramatically reversed by joint IL6 and GM-CSF blockade. A positive correlation between GM-CSF and IL6 expression and disease course was observed by meta-analyses of the clinical data.

Conclusions: Our studies indicate a significant reappraisal of the role of IL6 and GM-CSF in metastasis and implicate CAFs as the "henchmen" for cancer cells in producing an immunosuppressive tumor ecological niche. Dual targeting of GM-CSF and IL6 is a promising new approach for inhibiting metastasis. *Clin Cancer Res; 24(21); 5407–21. ©2018 AACR.*

Introduction

Metastatic cancer is a leading cause of death and significantly impacts on human health and society (1). Cancer rates are increasing as lifespan rises and lifestyles change in the developing world, potentiating the need to develop new therapeutics that target metastasis (2).

Metastasis in cancer cells is regulated by a complex interplay with noncancerous cells within the tumor ecological niche, which is mediated at a number of levels, including direct cell–cell communication, binding of extracellular matrix components and secreted factors, such as cytokines (reviewed in ref. 3). The network of cytokines in developing tumors has been termed "molecular cross-talk." This network has been the subject of intense investigation (e.g., refs. 4–7). However, the major players among these cytokines that promote tumorigenesis and metastasis are still undetermined because of the complexity of the multiple cellular interactions in the tumor ecological niche.

Tumor-associated macrophages (TAMs) have emerged as major regulators of cancer disease progression (8). TAMs derive from infiltrating monocytes or resident macrophages and are a major component of tumor-related inflammation. In broad terms, TAMs can be subdivided into two types: (i) classically activated, proinflammatory "M1" and (ii) alternatively activated, anti-inflammatory "M2" (9). Generally, during the early stages of tumor development, TAMs are predominantly the M1-like phenotype [e.g., inducible nitric oxide synthase (iNOS [NOS2])^{high}/arginase 1 (Arg-1)^{low}] and produce antitumorigenic mechanisms (10). In the later stages of tumor progression and metastasis, there is a greater presence of TAMs with marker expression profiles resembling the M2 phenotype (iNOS^{low}/Arg-1^{high}). These have been termed "M2-like" TAMs (8), which can promote tumorigenesis by secreting prometastatic cytokines, such as VEGF, IL1β, and EGF (10, 11).

[1]New Drug Targets Laboratory, School of Life Sciences, Gwangju Institute of Science and Technology, Gwangju, Republic of Korea. [2]School of Electrical Engineering and Computer Science, Gwangju Institute of Science and Technology, Gwangju, Republic of Korea. [3]Laboratory of *In Vivo* Molecular Imaging, Department of Nuclear Medicine, Chonnam National University Medical School and Hwasun Hospital, Gwangju, Republic of Korea. [4]Department of Oral Pathology, Oral Cancer Research Institute, Yonsei University College of Dentistry, Seoul, Republic of Korea.

Note: Supplementary data for this article are available at Clinical Cancer Research Online (http://clincancerres.aacrjournals.org/).

H. Cho and Y. Seo contributed equally to this article.

Corresponding Authors: Darren Reece Williams, Gwangju Institute of Science and Technology, Gwangju 61005, Republic of Korea (South). Phone: 826-2715-2509; Fax: 826-2715-2484; E-mail: darren@gist.ac.kr; and Da-Woon Jung, Gwangju Institute of Science and Technology, Gwangju 61005, Republic of Korea (South). Phone: 82-62-715-2509; Fax: 82-62-715-2484; E-mail: jung@gist.ac.kr

doi: 10.1158/1078-0432.CCR-18-0125

Translational Relevance

The differentiation and polarization of monocytes into M2 TAMs is an attractive therapeutic target, because M2 TAMs represent a crucial promoting force in solid tumor progression and metastasis. However, the complexity of regulatory cellular and molecular networks within the tumor microenvironment hampers the development of novel interventional strategies. We analyzed the multicellular cross-talk among cancer cells, CAFs, and monocytes that facilitate monocyte differentiation and polarization into protumoral TAMs. We found that CAFs have a key role in M2-like TAM induction via increased secretion of IL6 and GM-CSF in response to cancer cell stimulation. Furthermore, antibody blockade of IL6 and GM-CSF cooperatively reduced tumor growth and metastasis in an orthotopic syngeneic mouse model established by the coinjection of colon cancer cells and CAFs. Our study provides a comprehensive understanding of the major driving forces underlying macrophage polarization within the tumor microenvironment and also benefits the development of therapeutics for patients with cancer.

Cancer-associated fibroblasts (CAFs) constitute the most numerous noncancer cell type in tumors (12). These cells show great diversity in terms of their activation status, extracellular matrix (ECM) synthesis, and secretome (reviewed in ref. 13). CAFs act as the "henchmen" of cancer cells in the tumor microenvironment and promote tumorigenesis and metastasis by promoting cancer cell proliferation, enhancing angiogenesis, and modifying the ECM. The CAF secretome also regulates the composition of tumor-related inflammation, including the presence and phenotype of infiltrating TAMs (13). However, the molecular mechanisms by which CAFs promote monocyte differentiation into M2-like TAMs are not yet fully elucidated. This would provide valuable evidence that CAFs are a major target for antimetastatic therapeutics.

Given the crucial roles of CAFs and TAMs in dictating tumorigenesis and metastasis, we studied the three-way cross-talk between cancer cells and CAFs that promote monocyte differentiation into M2-like TAMs. Two cytokines, granulocyte macrophage colony-stimulating factor (GM-CSF/CSF-2) and IL6, showed increased expression by CAFs in response to cancer-CAFs cross-talk stimulation with cancer-derived cytokines, such as IL1α, and functioned as soluble factors that induced monocyte differentiation into M2-like TAMs. These findings indicate a reappraisal of our understanding about the roles played by GM-CSF and IL6 in developing tumors and implicate these cytokines as therapeutic targets for blocking the prometastatic cross-talk between CAFs, cancer cells, and tumor-infiltrating monocytes.

Materials and Methods

Reagents and antibodies

Recombinant human IL1α, human IL6, human IL7, human C-X-C motif chemokine 5 (CXCL5/ENA78), human GM-CSF/CSF2, recombinant mouse IL6, mouse GM-CSF, and human and mouse macrophage colony-stimulating factor (M-CSF/CSF1) were purchased from Prospec, Inc. Phorbol-12-myristate-13-acetate (PMA) and β-mercaptoethanol (β-ME) were purchased from Sigma. XenoLight D-Luciferin-K^+ Salt Bioluminescent Substrate was purchased from PerkinElmer. Collagen type I was purchased from Roche. The human cytokine antibody array C3 Kit was purchased from RayBiotech, Inc. Details of the antibodies used in this study can be found in Supplementary Table S2.

Cell culture

Human CAFs were derived from the oral cavity of 3 patients with oral squamous cell carcinoma (OSCC) and provided by Yonsei University College of Dentistry, Seoul, Republic of Korea. Normal fibroblasts were derived from a patient who underwent wisdom tooth extraction without mucosal disease. All studies involving human subjects were approved by the Institutional Review Board of Yonsei Dental Hospital, Yonsei University Health System. The studies were conducted in accordance with the Declaration of Helsinki. Written consent was obtained from each subject. CAFs were cultured in DMEM (Gibco) and Ham's Nutrient Mixture-F12 (Gibco) culture media at a ratio of 3:1 with 10% FBS (Gibco) and 1% penicillin/streptomycin (Gibco). The phenotype of CAFs compared with normal fibroblasts was verified by α-smooth muscle actin immunocytochemistry, effect on cancer cell invasion and upregulation of IL6 and GM-CSF expression after cancer cell stimulation (Supplementary Fig. S1).

THP-1 human monocytes, MDAMB231 human breast carcinoma cells, and HCT116 human colon carcinoma cells were obtained from the ATCC. YD-10B human oral squamous carcinoma cells were obtained from the Korean Cell Line Bank. THP-1 monocytes were maintained in RPMI1640 media (Gibco) supplemented with 10% FBS, 1% penicillin/streptomycin and 50 μmol/L β-ME. YD-10B cells were cultured in DMEM: Ham's-F12 (3:1) media supplemented with 10% FBS and 1% penicillin/streptomycin. HCT116 and MDAMB231 cells were cultured in DMEM supplemented with 10% FBS and 1% penicillin/streptomycin.

CT26-Luc murine colon carcinoma cells were a gift from Prof. Jung-Joon Min, Chonnam University Medical School, Republic of Korea, and cultured in DMEM supplemented with 10% FBS and 1% penicillin/streptomycin.

Human peripheral blood CD14-positive monocytes (PBMC) were obtained from iXCells Biotechnologies. The PBMC culture media were RPMI supplemented with 10% FBS, and 2 mmol/L L-glutamine. A total of 10 ng/mL recombinant human M-CSF was added depending on the experimental analysis. For macrophage induction, the culture media were changed to RPMI supplemented with 10% FBS, and 2 mmol/L L-glutamine, 1% sodium pyruvate + 1× nonessential amino acids, and 25 ng/mL human M-CSF.

Cell-based experiments were carried out within 2 months of thawing liquid nitrogen stocks. The cells used in this study were authenticated in 2018 by short tandem repeat DNA fingerprinting at the Korean Cell Line Bank, using the AmpFLSTR identifiler PCR Amplification Kit (Applied Biosystems) and the 3730 DNA Analyzer GeneMapper ID v3.2 databases (Applied Biosystems). The cell lines were routinely assessed for *Mycoplasma* contamination at the Animal House Core Facility of the Gwangju Institute of Science and Technology, Gwangju, Republic of Korea, using the e-Myco Mycoplasma PCR Detection Kit (Intron Biotechnology).

Collection of conditioned media

To obtain conditioned media (CM), cells were grown to subconfluence in 10-cm culture plates. The culture media were

changed to serum-free media. After 48 hours, the media were harvested, and debris was removed by centrifugation at 1,500 rpm for 3 minutes at 4°C.

Macrophage differentiation for THP-1

THP-1 monocytes were differentiated into macrophages by 72-hour treatment with 200 nmol/L PMA without β-ME in RPMI1640 media supplemented with 10% FBS, 1% penicillin/streptomycin, and employed as a positive control for macrophage differentiation experiments using CAF coculture, CM, or cytokines as stimuli.

Invasion assay

Cell invasion assays were performed using 24 transwell plates (Corning). The inserts containing 8-μm pore size filters were coated with collagen type I (45 μg/30 μL/well). A total of 2×10^4 cancer cells were seeded in the upper chamber with serum-free media. A total of 2×10^4 monocytes or macrophages were seeded in the lower chamber to compare proinvasive effects of the cells. After 48 hours, the cancer cells that penetrated the porous membrane were stained with 0.25 % crystal violet, documented with a light microscope, and quantified using ImageJ software (NIH, Bethesda, MD).

qPCR

The transcript level of cytokines was analyzed by qPCR using the StepOnePlus Real Time PCR System (Applied Biosystems). Cells were washed twice in PBS and frozen at −80°C until RNA isolation. Total RNA was isolated using TRIzol according to the manufacturer's protocol (Thermo Fisher Scientific) and mRNA was reverse transcribed to cDNA using the Improm-II reverse transcription system (Promega). The cDNA obtained was subjected to real-time PCR according to the manufacturer's instructions with the following modifications: qPCR was performed in triplicate in a total volume of 20 μL of 2× Power SYBR Green PCR Master Mix (Applied Biosystems) each containing 200 nmol/L (final concentration) of specific primer and 1 μL of cDNA. PCR amplification was preceded by incubation of the mixture for 10 minutes at 95°C and the amplification step consisted of 40 cycles of denaturation, annealing, and extension. Denaturation was performed for 15 seconds at 95°C, annealing was done for 1 minute at 60°C, and extension was performed at 72°C for 20 seconds with fluorescence detection at 72°C after each cycle. After the final cycle, melting point analysis of all of the samples was performed within the range of 60°C to 95°C with continuous fluorescence detection. A specific cDNA sample was included in each run and served as a reference for the comparison between runs. The data were normalized using the expression level of mouse *Actb* or human *ACTB* (β-actin). Results are expressed as the relative expression level of the gene in the experimental group compared with that of the control group. qPCR was performed with primer sets listed in Supplementary Table S3.

Western blotting

To analyze protein expression in adherent macrophages derived from THP-1 monocytes, the macrophages were scraped off the dish and transferred into a precooled microcentrifuge tube and resuspended in lysis buffer with protease inhibitors. To assess IL10 expression, macrophages were pretreated with 1× brefeldin A (1,000× for 5 mg/mL stock, BioLegend, Inc.) for intracellular accumulation of the cytokine 4 hours prior to protein extraction. Protein concentration was measured using the Bradford assay. The protein samples were loaded onto 10% (for CD206) or 15% (for IL10) polyacrylamide gels and transferred to 0.25 μm (for IL10) or 0.45 μm (for CD206) pore sized PVDF membranes after electrophoresis. Band intensities were visualized and quantified with ImageJ software.

ELISA

ELISA for serum, cell lysates, or tissue homogenates was performed using a commercial kit, according to the manufacturer's protocol (human IL6 and GM-CSF kits were purchased from R&D Systems, Inc.; mouse IL6 and GM-CSF were purchased from eBioscience). To analyze soluble levels of IL6 or GM-CSF, blood was collected from the tail vein of normal or tumor-bearing BALB/c mice, and CM were harvested after 48 hours of culture in serum-free media. To quantify cytokine levels in tissue homogenates, 10 to 30 mg tissue in 1 mL cold homogenization buffer (250 mmol/L sucrose, 1 mmol/L EDTA, 10 mmol/L Tris HCl buffer, pH 7.2 plus protease inhibitors) was homogenized using Wheaton Potter-Elvehjem Tissue Grinders with Teflon 0.25-inch diameter stainless steel rod pestles.

Cytokine antibody array

Cytokine expression levels were analyzed in cell supernatants using the human cytokine antibody array C3. A total of 2×10^5 CAFs were cultured in serum-free media with or without YD-10B CM (5%), after three washes with PBS. Twenty-four hours later, supernatants were harvested and analyzed using the cytokine array following the manufacturer's instructions.

Flow cytometry

Cells were harvested using TE solution, washed with PBS, and resuspended as a single-cell suspension. One-hundred microliters of the cell suspension containing 1×10^6 cells was added to each 5 mL flow cytometry tube (SPL Life Sciences; round bottom 5 mL tube). Antibodies were added for 15 minutes at room temperature in the dark. Cells were then washed 3 times by centrifugation at 1,500 rpm for 3 minutes and resuspended in ice-cold PBS. Flow cytometry was carried out using a BD FACSCanto II (BD Biosciences).

Animal studies

Animal experiments were approved by the Animal Care and Use Committees of the Gwangju Institute of Science and Technology (study approval number: GIST-2015-09). Mice were supplied by Damool Science.

Purification and culture of mouse bone marrow–derived monocytes

Mouse bone marrow–derived monocytes (BMDM) were isolated from the femur and tibia bones of 6- to 8-week-old C57BL/6 female mice, following the previously described protocol (14). The bone marrow cells were cultured on ultralow attachment 6-well plates for 5 days in RPMI1640 supplemented with 10% FBS, 1% penicillin/streptomycin, 2 mmol/L L-glutamine, 1× nonessential amino acids, 1 mol/L HEPES, 50 μmol/L β-ME, and 20 ng/mL M-CSF. BMDMs were purified by negative selection with anti-CD117 magnetic microbeads (Miltenyi Biotec) using a separator magnet to remove nonmonocyte cells from the cell population. As a positive and negative control for marker gene expression analysis, BMDMs were differentiated into M1-type or

M2-type macrophages by 3-day treatment with the following factors: 100 ng/mL GM-CSF, 10 ng/mL LPS plus 50 ng/mL murine IFNγ (for M1) or 100 ng/mL M-CSF and 10 ng/mL IL4 (for M2), as described previously (15).

Mouse CAF purification and culture

Tumor-bearing tissue containing murine CAFs was obtained from syngeneic tumor cell–injected mice, following the previously published protocols (16, 17). In brief, 10^5 CT26-Luc cells were injected subcutaneously into 6-week-old male BALB/c mice and tumors were allowed to develop for 3 to 4 weeks. Tissues surrounding the tumor were dissected into small pieces and digested using collagenase A (24.3 U/mL) and dispase II (125 U/mL). After filtering undigested tissues, the cell suspension was centrifuged at 2,000 rpm and the final pellet was resuspended in DMEM and seeded in a T25 culture flask. CAFs were maintained in DMEM and Ham's Nutrient Mixture-F12 culture media (1:1 ratio) supplemented with 15% FBS and 1% penicillin/streptomycin. Murine CAFs typically grew out of the tissue and were characterized by their morphology and *ACTA2* (α-SMA) expression compared with normal mouse fibroblasts.

Orthotopic syngeneic colon cancer mouse model

Six-week-old female BALB/c mice were maintained on an 8:16-hour light:dark cycle in an animal environmental control chamber. Eighty percent confluent cultures of CT26-Luc cells were harvested using 0.05% trypsin-EDTA solution, washed in PBS, and resuspended in PBS. General anesthesia in mice was performed using a combination of ketamine (22 mg/kg) and xylometazoline (10 mg/kg) in PBS injected intraperitoneally. The abdominal cavity was opened with a 7- to 8-mm median laparotomy exposing the cecum. A total of 5×10^4 CT26-Luc cells with/without 1.5×10^5 mouse-derived CAF cells (1:3 ratio) were suspended in 50 μL DMEM and carefully injected under the serosa of the cecum wall of the syngeneic BALB/c mice using a 27-gauge needle. The cecum was then replaced into the abdominal cavity, and the laparotomy was closed by a two-layer closure of the peritoneum and skin using 5-0 nylon sutures (Ailee Co., Ltd).

Tumor-bearing mice were anaesthetized by isopantane inhalation, and tumor growth was monitored using an *in vivo* imaging system (Caliper IVIS Kinetic In Vivo Optical Imaging System) after luciferin injection (150 μL/mouse from a 15 mg/mL stock solution). The photon flux of each mouse was measured using Living Image software 3.1 (Xenogen). Tumor size (width (w) and length (L)) was calculated using the following formula:

$$\text{Tumor size} = \frac{(\text{w})^2 \times \text{L}}{2}$$

The metastasis rate was assessed using the previously described methodology (18), based on monitoring bioluminescence using IVIS after luciferin injection. For the antibody blockade study, mice were pretreated with intraperitoneal injections of 100 μg/mouse anti-IL6 and/or 100 μg/mouse anti–GM-CSF dissolved in PBS prior to cancer cell transplantation. After transplantation, the mice were treated with 100 μg/mouse anti-IL6 and/or 100 μg/mouse anti–GM-CSF twice per week and sacrificed at 6 weeks' posttransplantation.

Immunocytochemistry

CAFs were cultured on chamber slides (Sigma) for 24 hours. Cells were then immunostained for α-SMA, a myofibroblast marker, and an activated cancer-associated fibroblast marker. Alexa Fluor 488 goat anti-mouse IgG was used as a secondary antibody (Invitrogen). Nuclei were stained using ProLong Gold antifade reagent (DAPI Mounting, Life Technologies). Staining was visualized by fluorescence microscopy (Leica DMI3000 B).

IHC

Tumor-bearing mouse colon tissues were prefixed in 4% formaldehyde solution in 1× PBS at 4°C for 24 hours and sequentially incubated with 15% and 30% sucrose solution in 1× PBS at 4°C until the tissues sink into the solution. For cryosectioning, tissues were frozen in OCT solution (Leica) and 10- to 12-μm sections were cut with a Leica CM1900 cryostat. The section on the slide was air-dried before staining and permeabilized using 0.1% Triton X-100 in PBS for 10 minutes. For IHC staining, the slides were washed using TBST solution (TBS with 0.025% Triton X-100) with gentle agitation and then blocked in 10% normal goat serum (from the species in which the secondary was raised) with 1% BSA in TBS for 2 hours at room temperature (including 0.3 mol/L glycine). Slides were drained for a few seconds and wiped around the sections with tissue paper. Tissue sections were incubated with the antibodies overnight at 4°C. For fluorescent detection, secondary antibodies were applied using a fluorophore-conjugated secondary Ab (goat anti-rabbit IgG-heavy and light chain antibody DyLight594 conjugated or goat anti-mouse IgG-heavy and light chain antibody DyLight594 conjugated) to the slide diluted in TBS with 1% BSA and incubated for 1 hour at room temperature in the dark. Stained sections were mounted using compatible mounting medium including DAPI. For evaluation of IHC, stained colon tissues were visualized with the Lionheart FX Automated Microscope (BioTek, Inc.) in 10 high-power fields at 200× and the double-stained cells ($CD68^+$, $CD86^+$, or $CD206^+$) were analyzed and counted using Gen5 software (BioTek, Inc.)

Meta-analysis of GM-CSF and IL6 expression in patient tumor tissues

GM-CSF and IL6 expressions in head and neck cancer and colorectal cancer patient cases were analyzed and compared using the Oncomine Online Database (https://www.oncomine.org/resource/login.html).

Statistical analysis

Statistical analysis was carried out using Excel (Microsoft) and GraphPad Prism 6 (GraphPad software, Inc). The parametric Student *t* test was used for statistical analysis of the cell-based experiments. The nonparametric Mann–Whitney *U* test was used for statistical analysis of the animal-based experiments. The χ^2 test was used for statistical analysis of metastasis.

Results

CAFs secrete factors that induce human monocyte differentiation into proinvasive, M2-like macrophages

To test the effect of CAFs on monocyte differentiation, human CAFs from patients with OSCC were cocultured with THP-1 human monocytes. The effect of CAFs was compared with PMA (a known inducer of macrophage differentiation). CAFs induced

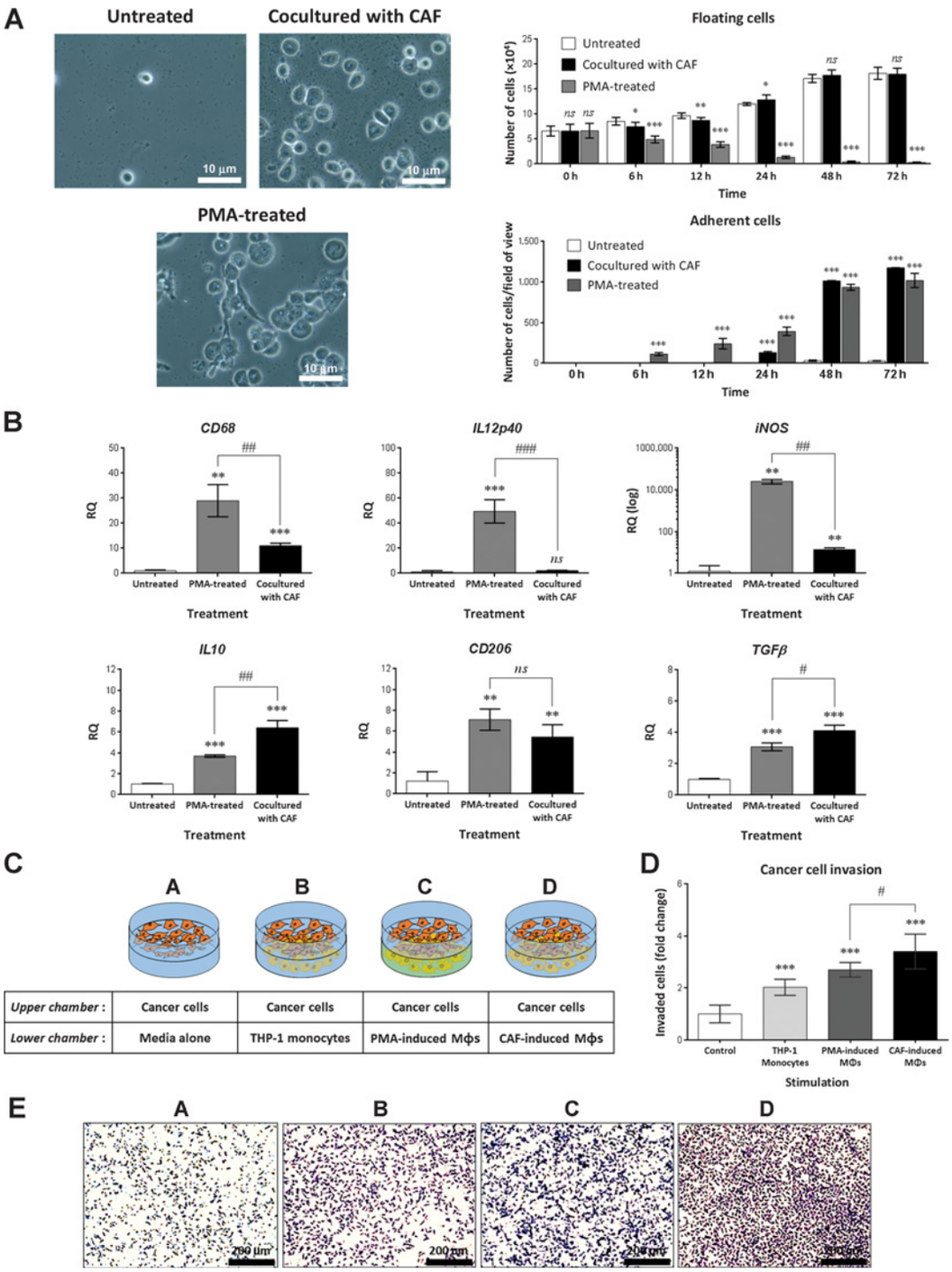

Figure 1.

CAFs induce monocyte differentiation into proinvasive macrophages with M2-like characteristics. **A,** 6×10^4 THP-1 human monocytes were cocultured with 2×10^4 human OSCC CAFs in a 24 transwell system (pore size, 0.4 μm) or treated with 200 nmol/L PMA (a known inducer of differentiation) for 72 hours. Micrographs indicated that treatment with PMA or coculture with CAFs increased monocyte differentiation into adherent macrophages. Scale bar, 10 μm. The increase in differentiation was quantified by counting cells that adhered to the culture plate. $n = 3$; error, SD. **B,** qPCR analysis of *CD68* (pan-macrophage marker); *IL12p40* and *iNOS* (M1 markers); *IL10*, *CD206*, and *TGFβ* (M2 markers) in the adherent macrophages. *ACTB* (human β-actin) was used to normalize gene expression. $n = 3$; error, SE. **C,** Schematic diagram of the protocol to measure the effect of CAF-induced macrophages on cancer cell invasion. $n = 3$; error, SE. **D,** Invasion assay for 2×10^4 YD-10B cancer cells alone (**A**) or with the following cells types: THP-1 monocytes (**B**), macrophages produced by treating THP-1 monocytes with PMA (**C**), and macrophages produced by coculturing THP-1 monocytes with CAFs (**D**). **E,** Representative micrographs of crystal violet–stained invaded cells. Scale bar, 200 μm; ns, not significant; *, $P < 0.05$; **, $P < 0.01$; ***, $P < 0.001$; #, $P < 0.05$; ##, $P < 0.01$; ###, $P < 0.001$.

monocyte differentiation into macrophages, as indicated by increased adhesion to the culture plate, whereas floating cell numbers of THP-1 were not significantly changed compared with the control at the 48- and 72-hour time points (Fig. 1A). To assess the phenotype of the differentiated macrophages, the expression of M1- and M2-related markers was measured by real-time PCR. Macrophages produced by PMA treatment or coculture with CAFs showed increased expression of the pan-macrophage marker *CD68* and the M2 marker *CD206* (Fig. 1B; ref. 19). In contrast, macrophages produced by coculture with CAFs showed relatively high expression of the M2 markers *IL10* and *TGFB1* (*TGFβ*; ref. 20) and relatively low expression of the M1 markers IL12 subunit p40 (*IL12p40*) and *iNOS* (21), compared with macrophages produced by PMA treatment (Fig. 1B).

In addition, the effects of these macrophages on cancer cell invasion were assessed. Compared with THP-1 monocytes or PMA-induced macrophages, the macrophages derived by coculturing with CAFs induced higher levels of cancer cell invasion (Fig. 1C–E).

Cancer cells stimulate human CAFs to potentiate monocyte differentiation into M2-like macrophages

To model the three-way cross-talk between cancer cells, CAFs, and monocytes in the tumor ecological niche, CM was collected from human OSCC cancer cells (YD-10B) and treated to cocultures of CAFs and human monocytes. The effect on monocyte differentiation was compared with THP-1 monocytes treated with YD-10B CM alone, or THP-1 monocytes cocultured with OSCC CAFs (Fig. 2A). Interestingly, addition of diluted cancer cell CM to the monocyte–CAF cocultures showed synergistic effects on monocyte differentiation (number of adherent cells) compared with cancer CM alone or coculturing with CAFs (Fig. 2B and C). We hypothesized that inducible factors are present in the CAFs that increase monocyte differentiation. To check that this effect was not restricted to just one cancer cell type, the CM from HCT116 colon carcinoma or MDAMB231 breast carcinoma cells was tested. Addition of the diluted cancer cell CM to monocyte–CAF cocultures also produced higher levels of differentiation, compared with monocytes treated with cancer cell CM alone or CAF CM alone (Fig. 2D). This finding indicated the existence of inducible factors in the CAFs that respond to cancer cell CM and promote monocyte differentiation. To investigate whether cancer CM-stimulated CAFs can promote the M2-like phenotype, THP-1 monocytes were treated with a mixture of YD-10B CM (5%) and CAF CM (5%), or YD-10B CM-stimulated CAF CM. After 72 hours, CD206 and IL10 expression was analyzed by Western blotting. The CM from CAFs stimulated with cancer cell CM was markedly more effective than the CAF and cancer cell CM mixture at inducing monocyte differentiation into M2-like macrophages, as shown by increased expression of the M2 markers IL10 and CD206 (Fig. 2E and F). Expression of the members of the STAT family have also been linked with macrophage polarization, with higher levels of *STAT1* in M1 macrophages and higher levels of *STAT3* in M2 macrophages (22). Macrophages produced by cancer-activated CAF CM treatment showed a higher ratio of *STAT3*:*STAT1* expression compared with macrophages produced by PMA, indicating a more M2-like phenotype in the macrophages produced by CM treatment (Supplementary Fig. S2). This result further indicated the presence of cancer cell–inducible factors in CAFs that promote monocyte differentiation into M2-like macrophages.

Cancer cells increase the secretion of GM-CSF and IL6 from CAFs to promote monocyte differentiation

To identity the inducible factors secreted by cancer cell–stimulated CAFs that drive monocyte differentiation into M2-like macrophages, the cytokine array was performed. Cancer cell CM stimulated CAFs upregulated secretion of the cytokines CXCL1, CXCL5, M-CSF, GM-CSF, IL6, IL7, CCL5, CCL7, and CCL8, compared with CAFs alone (Fig. 3A). The cytokines IL6, IL7, CXCL5, and GM-CSF showed significant increases in secretion (statistical threshold set as a 5-fold increase; Supplementary Fig. S3) and were not previously known as promigratory factors and, therefore, may influence monocyte adherence or differentiation. Our previous study indicated that IL1α is a key mediator of the proinvasive cross-talk between cancer cells and CAFs (6). Cytokine array analysis of IL1α-stimulated CAFs also detected an increase in the secretion of IL6, CXCL5, and GM-CSF (Supplementary Fig. S4). Therefore, IL6, IL7, CXCL5, and GM-CSF were selected for further analysis of their effects on monocyte differentiation. IL6 and GM-CSF, but not IL7 and CXCL5, could induce monocyte differentiation (Fig. 3B and C). ELISA analysis confirmed that the ability to induce GM-CSF and IL6 secretion in CAFs is a feature of cancer cell CM from different tumor types, such as colon and breast carcinoma (Fig. 3D). It should be noted that the MDAMB231 breast carcinoma cell CM already contained detectable levels of GM-CSF, which was further increased by coculture with CAF. Further analysis showed that IL6 and GM-CSF induced monocyte differentiation at the 12.5 ng/mL concentration, whereas IL7 and CXCL5 had no effect up to the 50 ng/mL concentration (Supplementary Fig. S5). Time course analysis of 4 different time points (12, 24, 48, and 72 hours) indicated that greatest differences in adhesion could be observed at the 72-hour time point (Supplementary Fig. S6).

IL6 and GM-CSF cooperatively induce monocyte differentiation into M2-like, proinvasive macrophages

The phenotype of macrophages produced by IL6 and GM-CSF was assessed using cancer cell invasion assays and marker expression analyses. Macrophages produced by IL6 or GM-CSF treatment increased cancer cell invasion (Fig. 3E). Marker analysis showed that macrophages produced by IL6 treatment increased expression of the macrophage marker *CD68* and the M2 markers *CD206*, *Arg-1*, and *TGFβ* (Supplementary Fig. S7A). In contrast, macrophages produced by GM-CSF showed increased expression of *CD68*, *CD206*, *Arg-1*, and *TGFβ*, along with increased expression of the M1 markers *IL12p40* and *iNOS*. Combined treatment with GM-CSF and IL6 reduced the expression of *IL12p40* and increased the expression of *CD206*, *Arg-1*, and *TGFβ* compared with GM-CSF treatment alone (Supplementary Fig. S7A).

Human $CD14^+$ PBMCs were used to investigate the effects of IL6 and/or GM-CSF on human monocyte differentiation after priming with M-CSF, in accordance with the recommended guidelines for human PBMC differentiation into macrophages (15). Pan-macrophage (CD11b), M1 (CD86), and M2 (CD206) marker expression was measured using flow cytometry (Supplementary Fig. S7B). IL6 treatment increased the proportion of $CD11b^+$, $CD206^+$, and $CD86^-$ macrophages. GM-CSF treatment had a reduced effect on differentiation into $CD11b^+$, $CD206^+$, and $CD86^-$ macrophages. In contrast, combined treatment with IL6 and GM-CSF increased differentiation into $CD11b^+$, $CD206^+$, and $CD86^-$ macrophages, which is

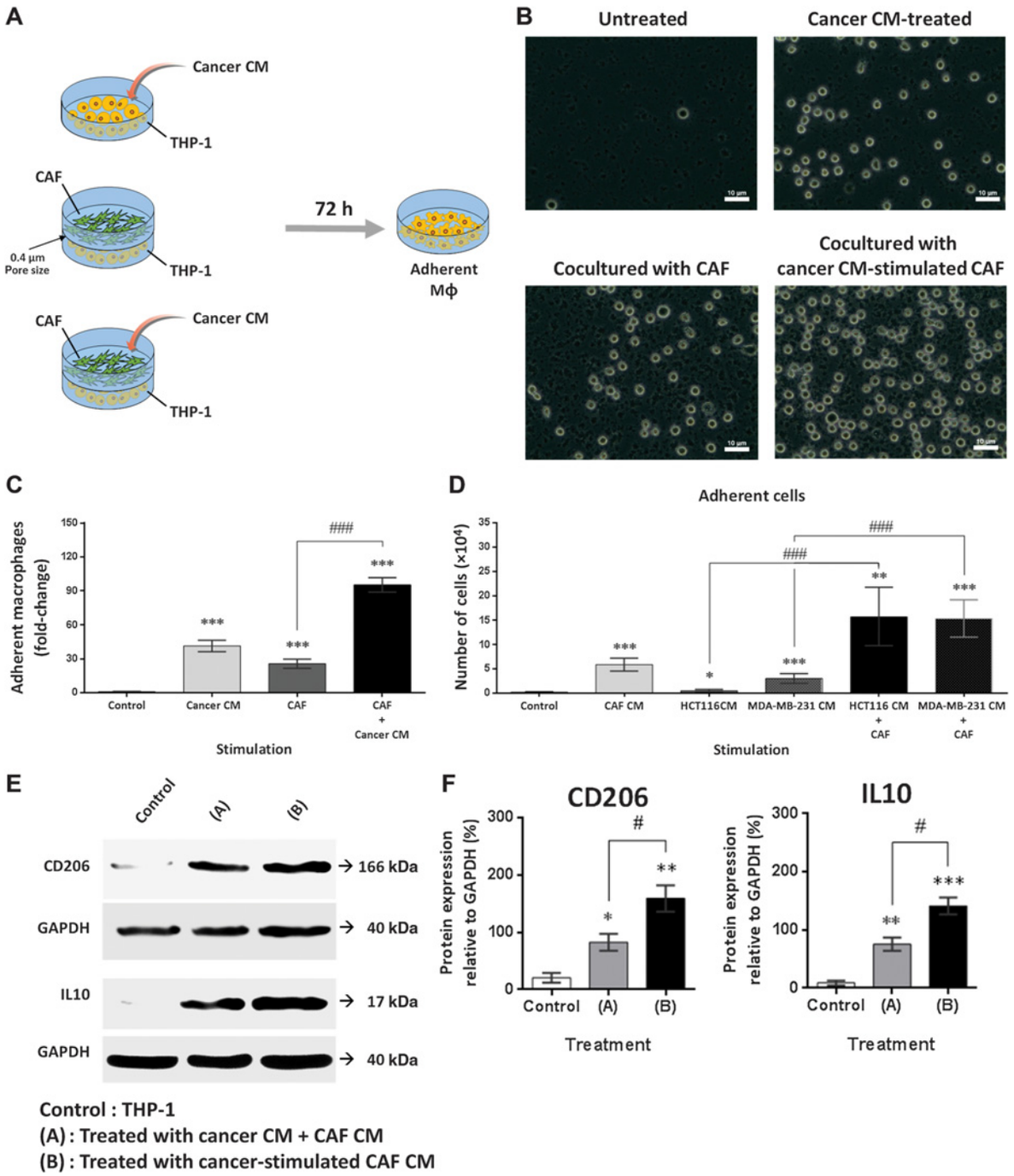

Figure 2.

Cancer cells potentiate CAF-induced monocyte differentiation into M2-like macrophages. **A,** Schematic diagram of the transwell systems used to investigate the effect of cancer CM-stimulated CAFs on monocyte differentiation. **B,** A total of 2×10^5 THP-1 monocytes treated with the following stimuli: (i) YD-10B CM (5% final concentration); (ii) coculturing with 2×10^4 CAFs; (iii) coculturing with 2×10^4 CAFs plus YD-10B CM (5% final concentration), underwent differentiation into adherent macrophages. Addition of cancer cell CM to CAF–monocyte cocultures induced significantly higher levels of monocyte differentiation compared with coculturing without cancer CM (scale bar, 10 μm). **C,** Quantification of macrophages differentiated by the above conditions. $n = 3$; error, SE. **D,** Effect of HCT116 colon carcinoma or MDAMB231 breast carcinoma cell CM on CAF-induced THP-1 monocyte differentiation. THP-1 was treated with cancer CM alone or cocultured with CAFs in the absence or presence of cancer CM for 72 hours. $n = 9$; error, SD. **E,** Western blotting for M2 marker expression (CD206, 166 kDa and IL10, 17 kDa) in the differentiated macrophages. THP-1 monocytes were treated with a mixture of YD-10B cancer cell CM and CAF CM, or CM from YD-10B CM stimulated CAFs, for 72 hours. **F,** Quantification of CD206 and IL10 expression in the differentiated macrophages. $n = 4$; error, SD. ns, not significant; *, $P < 0.05$; **, $P < 0.01$; ***, $P < 0.001$; #, $P < 0.05$; ###, $P < 0.001$.

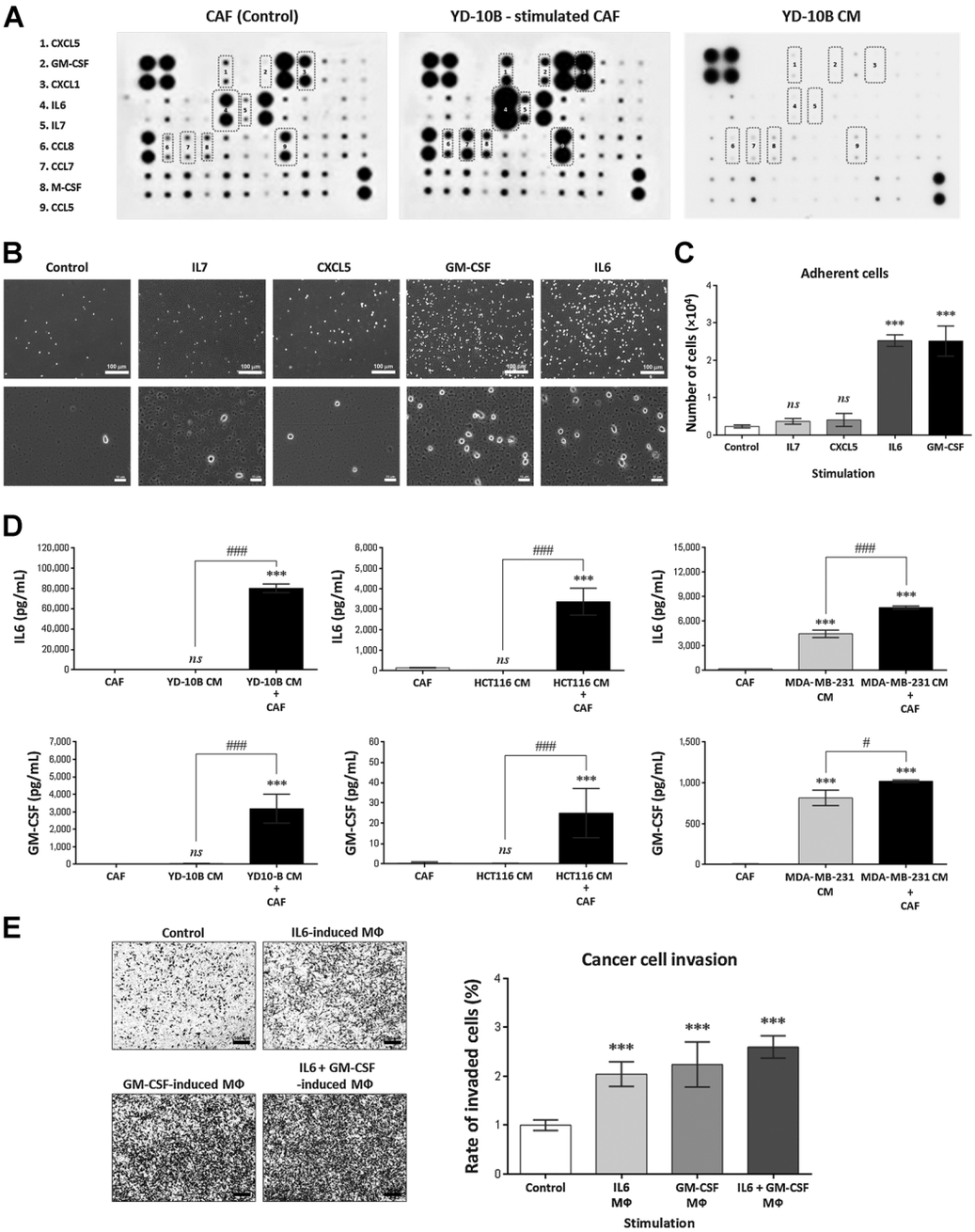

Figure 3.

GM-CSF and IL6 are the factors secreted by cancer cell–stimulated CAFs that induce monocyte differentiation. **A,** Human cytokine array for CAF culture supernatant, CAF culture supernatant after YD-10B cancer CM stimulation, and YD-10B CM. Cytokines upregulated in cancer-stimulated CAFs are indicated with red boxes. **B,** Representative photographs of THP-1 monocyte differentiation into macrophages after treatment with 12.5 ng/mL IL7, CXCL5, GM-CSF, or IL6 for 72 hours (scale bar, 100 μm for low-magnification pictures and 10 μm for high-magnification pictures). **C,** Quantification of THP-1 monocyte differentiation into macrophages after cytokine treatment. $n = 3$; error, SE. **D,** GM-CSF and IL6 secretion by CAFs after treatment with CM from different cancer cell types. CAFs were treated with CM from YD-10B OSCC cells, HCT116 colon carcinoma cells, or MDAMB231 breast carcinoma cells for 24 hours. GM-CSF or IL6 secretion was measured by ELISA. $n = 3$; error, SD. **E,** Invasion assay for YD-10B cells alone (control) or YD-10B cells cocultured with macrophages derived from THP-1 monocytes by treatment with 12.5 ng/mL IL6, 12.5 ng/mL GM-CSF, or 12.5 ng/mL IL6 + 12.5 ng/mL GM-CSF (scale bar, 100 μm). $n = 3$; error, SD. ns, not significant; ***, $P < 0.001$; #, $P < 0.05$; ###, $P < 0.001$.

broadly in concurrence with the M2 marker expression pattern for *CD206* and *Arg-1* observed in the THP-1–derived macrophages (Supplementary Fig. S7A and S7B).

The effects of IL6 and GM-CSF on macrophage polarization were further investigated using BMDMs (Fig. 4A). Pretreatment with M-CSF has been used to prime BMDMs for differentiation (15). Therefore, we investigated the effects of GM-CSF and IL6 on BMDM differentiation in the presence or absence of M-CSF. Both GM-CSF and IL6 increased BMDM differentiation (Fig. 4B). Marker analysis indicated that IL6 treatment increased expression of the murine macrophage marker ADGRE1 (F4/80) (Supplementary Fig. S8). Treatment with GM-CSF increased the expression of *ADGRE1* (*F4/80*) and the M1 markers *iNOS* and *IL12p40*, and also increased expression of the M2 markers IL10 and Arg-1. Treatment with GM-CSF and IL6 together reduced expression of the M1 markers, IL12p40 and iNOS, compared with GM-CSF treatment alone, which is consistent with the THP-1 monocyte study (Supplementary Fig. S7A). In the M-CSF culture condition, combined treatment with GM-CSF and IL6 increased the *Arg-1/iNOS* expression ratio, indicating an M2-like phenotype, compared with GM-CSF treatment alone. Macrophages produced by IL6 treatment also showed a higher ratio of *STAT3:STAT1* expression compared with macrophages derived by GM-CSF treatment, indicating a more M2-like phenotype in macrophages produced by IL6 treatment (Supplementary Fig. S9). IL6 also inhibited the induction of *STAT1* by GM-CSF. Furthermore, macrophages differentiated from BMDMs by treatment with IL6 and GM-CSF increased cancer cell invasiveness to a similar degree as that produced by M2-type macrophages (Supplementary Fig. S10). Flow cytometry analysis of CD11b (pan-macrophage), CD206 (M2 marker), and CD86 (M1 marker) expression showed that, compared with control cells, treatment with IL6 or GM-CSF increased differentiation into $CD11b^+$ $CD206^+$ $CD86^-$ macrophages. Combined treatment of IL6 and GM-CSF further increased differentiation into $CD11b^+$ $CD206^+$ $CD86^-$ macrophages (Fig. 4C).

Primary murine CAFs upregulate GM-CSF and IL6 secretion in response to cancer cell stimulation

To assess whether GM-CSF and IL6 secretion is upregulated in cancer cell CM-stimulated CAFs *in vivo*, CAFs were purified from a syngeneic model of colon carcinoma, as described previously (Fig. 5A; refs. 16, 17). Murine CAFs were identified by increased expression of α-SMA compared with normal fibroblasts (Supplementary Fig. S11A and S11B). The purified CAFs also enhanced cancer cell invasiveness compared with normal fibroblasts (Supplementary Fig. S11C). After stimulation with CM from CT26 murine colon cancer cells, the CAFs upregulated secretion of IL6 and GM-CSF (Supplementary Fig. S11D).

Primary murine CAFs cotransplanted with CT26 colon cancer cells promote tumorigenesis and metastasis, increase GM-CSF and IL6 levels, and M2-like macrophage infiltration

The relationship between cotransplanted CAFs, M2-like TAM infiltration, progression to colon cancer metastasis, and the expression of IL6 and GM-CSF was investigated *in vivo* using an orthotopic syngeneic tumor model (Fig. 5B). Animals transplanted with colon carcinoma cells and CAFs showed a significant increase in tumor photon flux compared with animals transplanted with cancer cells alone (Fig. 5C and D). Animals cotransplanted with CAFs plus cancer cells also showed faster tumor development and spread. After sacrifice, primary tumor weight and liver weight were significantly greater in the cotransplanted group (Fig. 5E and F; Supplementary Fig. S12). Animals cotransplanted with cancer cells and CAFs also showed a greater rate of metastasis as detected by IVIS imaging and assessment of liver tissue (Supplementary Fig. S13). ELISA at 3 and 6 weeks post-transplantation showed that cotransplantation of CAFs with cancer cells produced higher serum levels of IL6 (at both time points) and GM-CSF (at 6 weeks; Fig. 5G). Increased expression of IL6 and GM-CSF was also detected in the tumors from cotransplanted mice (Supplementary Fig. S14). IHC analysis of CD68 and CD206 showed that tumors derived from carcinoma cells cotransplanted with CAFs contained higher numbers of infiltrating M2-like macrophages compared with tumors derived from transplanted carcinoma cells alone (Supplementary Fig. S15).

GM-CSF and IL6 is upregulated in patients with head/neck and colorectal cancer

To assess whether GM-CSF and IL6 are upregulated factors in cancer, the expression level in patients was investigated using the Oncomine database (https://www.oncomine.org). Head/neck cancer and colorectal cancer were selected for analysis because our experiments mainly utilized oral carcinoma and colon carcinoma cells. GM-CSF and IL6 were found to be upregulated in the listed patient datasets compared with normal tissue (Supplementary Table S1). IL6 was also found to be upregulated in a disease stage–dependent manner in the Bittner colon and TCGA COAD databases, whereas GM-CSF was also found to be upregulated in a disease stage–dependent manner in the TCGA HNSC (oral cancer) database (Supplementary Table S1).

Antibody blockade of GM-CSF and IL6 inhibits tumorigenesis and metastasis of colon cancer *in vivo*

The role of GM-CSF and IL6 in monocyte differentiation into M2-like macrophages was investigated using antibody blockade. THP-1 monocytes were treated with antibodies against IL6 and/or GM-CSF in the presence of cancer cell–stimulated CAF CM. Antibody treatment inhibited the expression of *IL10*, *CD68*, and *Arg-1* in THP-1–derived macrophages *in vitro*, indicating reduced differentiation into M2-like macrophages (Supplementary Fig. S16).

In the syngeneic, orthotopic colon carcinoma model, blockade with IL6 antibody (100 μg/mouse) and/or GM-CSF antibody (100 μg/mouse) reduced tumorigenesis, as indicated by lower photon flux from the cancer cells and reduced tumor spread (Supplementary Fig. S17; Fig. 6A and B). Antibody blockade also reduced primary tumor weight (Fig. 6C). Furthermore, blockade with IL6 and GM-CSF antibodies together produced a greater inhibitory effect on photon flux and tumor size and weight (Fig. 6A–C; Supplementary Fig. S18), and lung and liver metastasis (Fig. 6D and E; Supplementary Fig. S19). IHC assessment of CD86 (M1 marker) and CD206 (M2 marker) expression in the tumor tissue indicated that antibody treatment increased the presence of M1 macrophages (Supplementary Fig. S20) and reduced the number of M2 macrophages (Fig. 6F and G).

The effects of a 50 or 200 μg antibody blockade dose were also investigated (Supplementary Fig. S21). It was observed that the 200 μg dose did not significantly affect overall survival, even though tumor growth was significantly reduced at 3 weeks, (Supplementary Fig. S21A and S21B), presumably due to toxicity

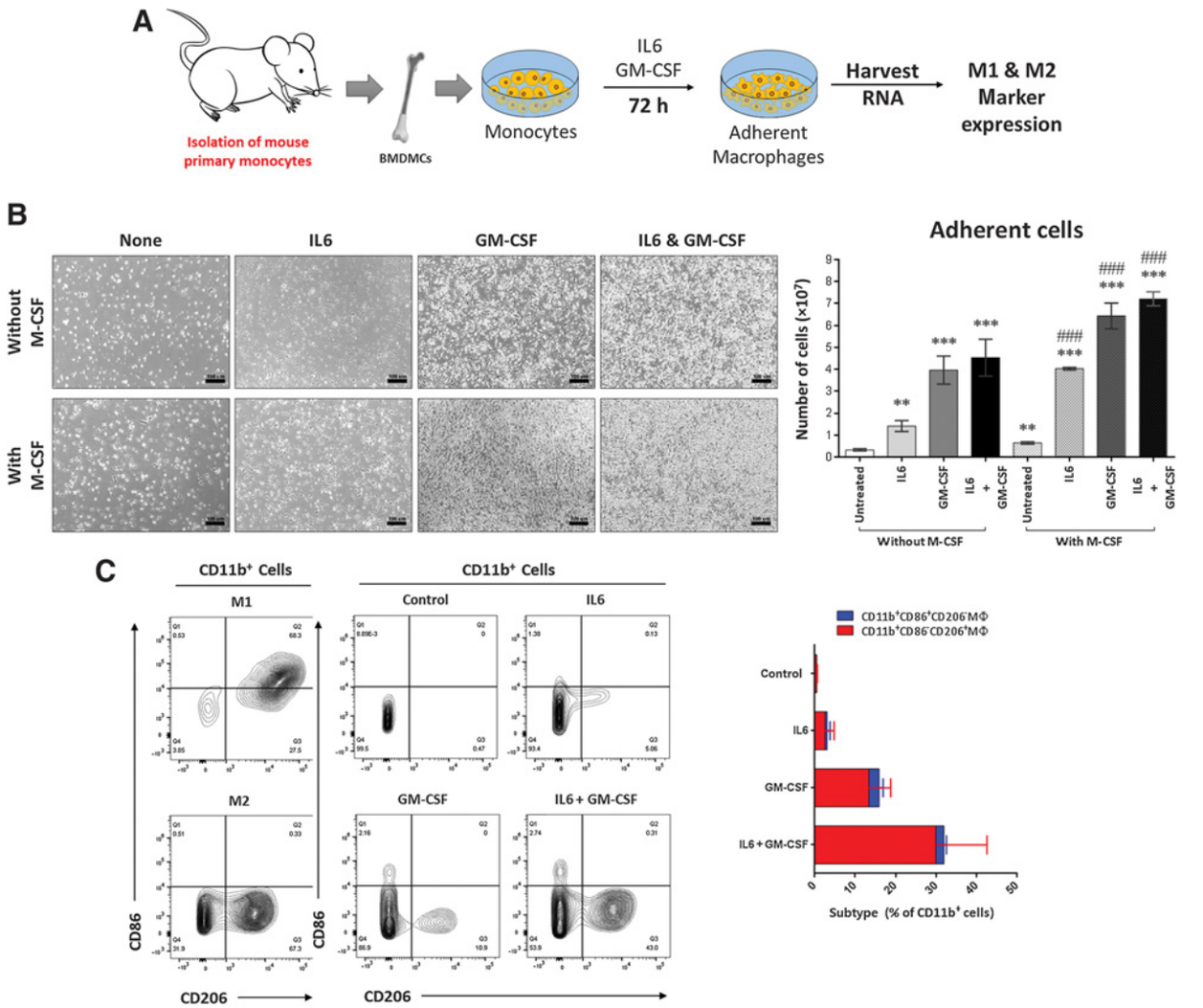

Figure 4.

GM-CSF and IL6 induce BMDM differentiation into proinvasive M2-like macrophages. **A,** Schematic diagram of the protocol assessing the effect of GM-CSF and/or IL6 on BMDM differentiation. **B,** Micrographs of 2×10^4 BMDMs after treatment with 12.5 ng/mL GM-CSF and/or 12.5 ng/mL IL6 for 72 hours. Scale bar, 100 μm. The bar chart shows quantification of BMDM differentiation by counting adherent macrophages. The effect of 20 ng/mL M-CSF treatment (a recommended protocol for monocyte purification from bone marrow cells; ref. 15) was also assessed. $n = 3$; error, SE. **C,** Flow cytometry analysis of CD86 (M1 marker), CD11b (M1/M2 marker), and CD206 (M2 marker) expression in the BMDMs after cytokine treatment. The bar chart shows the quantification of the $CD11b^+$, $CD86^+$, and $CD206^-$ (M1) population and $CD11b^+$, $CD86^-$, and $CD206^+$ (M2) populations. $n = 3$; error, SD. **, $P < 0.01$ and ***, $P < 0.001$ (compared to untreated control w/o M-CSF); ###, $P < 0.001$ (compared to untreated control with M-CSF).

associated with the 200 μg dose. Both doses of the antibody could reduce metastasis in the mice that survived the time course of the experiment (Supplementary Fig. S21C).

Discussion

TAMs are attractive treatment targets in clinical oncology (8). The role of CAFs in regulating monocyte differentiation into TAMs has not been fully elucidated. Identifying the factors that regulate this differentiation can provide new targets for anti-cancer therapeutics. These factors can be classified "afferent" (arising from the cancer cell) or "efferent" (arising from the cancer-activated CAFs). In this study, we characterized inducible, efferent factors in CAFs that respond to afferent factors from cancer cells and promote monocyte differentiation into proinvasive TAMs. We discovered that GM-CSF and IL6 are efferent factors in CAFs that promote this differentiation and, in turn, enhance TAM-induced cancer cell invasion *in vitro*. This triple cross-talk between cancer cells, CAFs, and monocytes, mediated by CAF-derived GM-CSF and IL6, regulates the presence of proinvasive TAMs in developing tumors and the progression to metastasis. Thus, IL6 and GM-CSF are important targets for modulating the interaction between TAMs and CAFs that regulate tumor-associated inflammation. Although our

in vitro system used OSCC cells to identify IL6 and GM-CSF, we extended these findings to an additional cancer type, colon carcinoma, using animal models.

To characterize the interplay between cancer cells, CAFs, and monocytes, we stimulated CAFs with cancer cell CM. This model was used to identify chemokine CCL7 as the CAF-derived factor

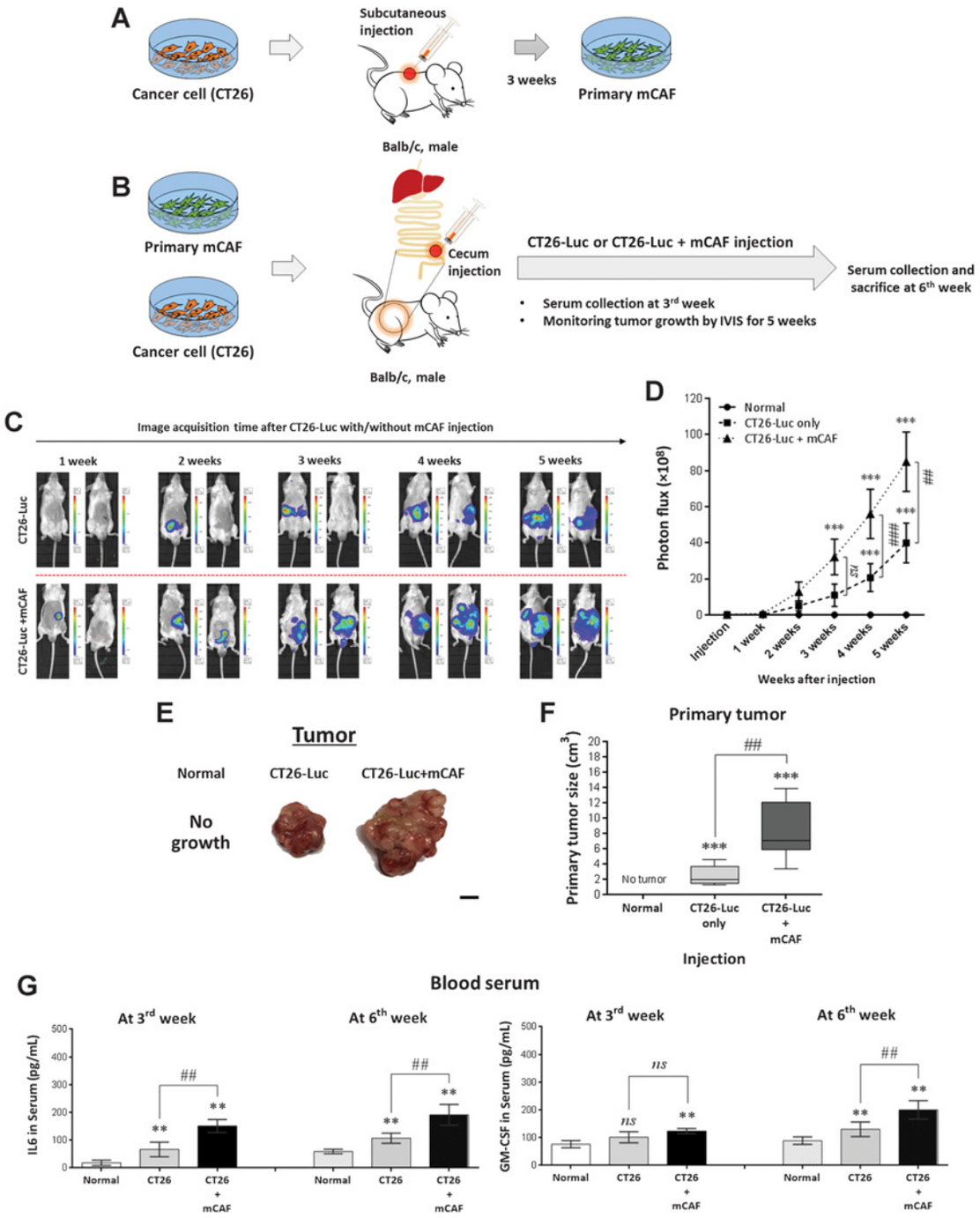

Figure 5.

CAFs enhance cancer cell invasion, facilitate metastasis, and increase serum/tumor levels of IL6 and GM-CSF in an orthotopic, syngeneic colon carcinoma model. **A,** Schematic diagram showing the isolation of primary CAFs. **B,** Schematic diagram of the protocol to investigate the effect of CAFs on CT26 murine colon cancer cell metastasis and IL6 and GM-CSF expression levels. **C,** IVIS images of representative mice during the 5 weeks' time course posttransplantation. **D,** Photon flux detected from cancer cells in the transplanted mice. $n = 8$ mice/group; error, SE. **E,** Representative photographs of the tumors at 6 weeks' posttransplantation. **F,** Bar chart of primary tumor size. $n = 8$ mice/group; error, SE. **G,** ELISA for serum levels of IL6 and GM-CSF. $n = 6$; error, SE. ns, not significant; **, $P < 0.01$; ***, $P < 0.001$; ##, $P < 0.01$; ###, $P < 0.001$.

promoting OSCC invasion in response to IL1α secretion in the tumor ecological niche (6). Our results show that monocytes cocultured with human CAFs differentiated into macrophages that enhanced cancer cell invasion (Fig. 1A–E). The addition of cancer cell CM to monocyte–CAF cocultures induced higher levels of monocyte differentiation, compared with CM addition to

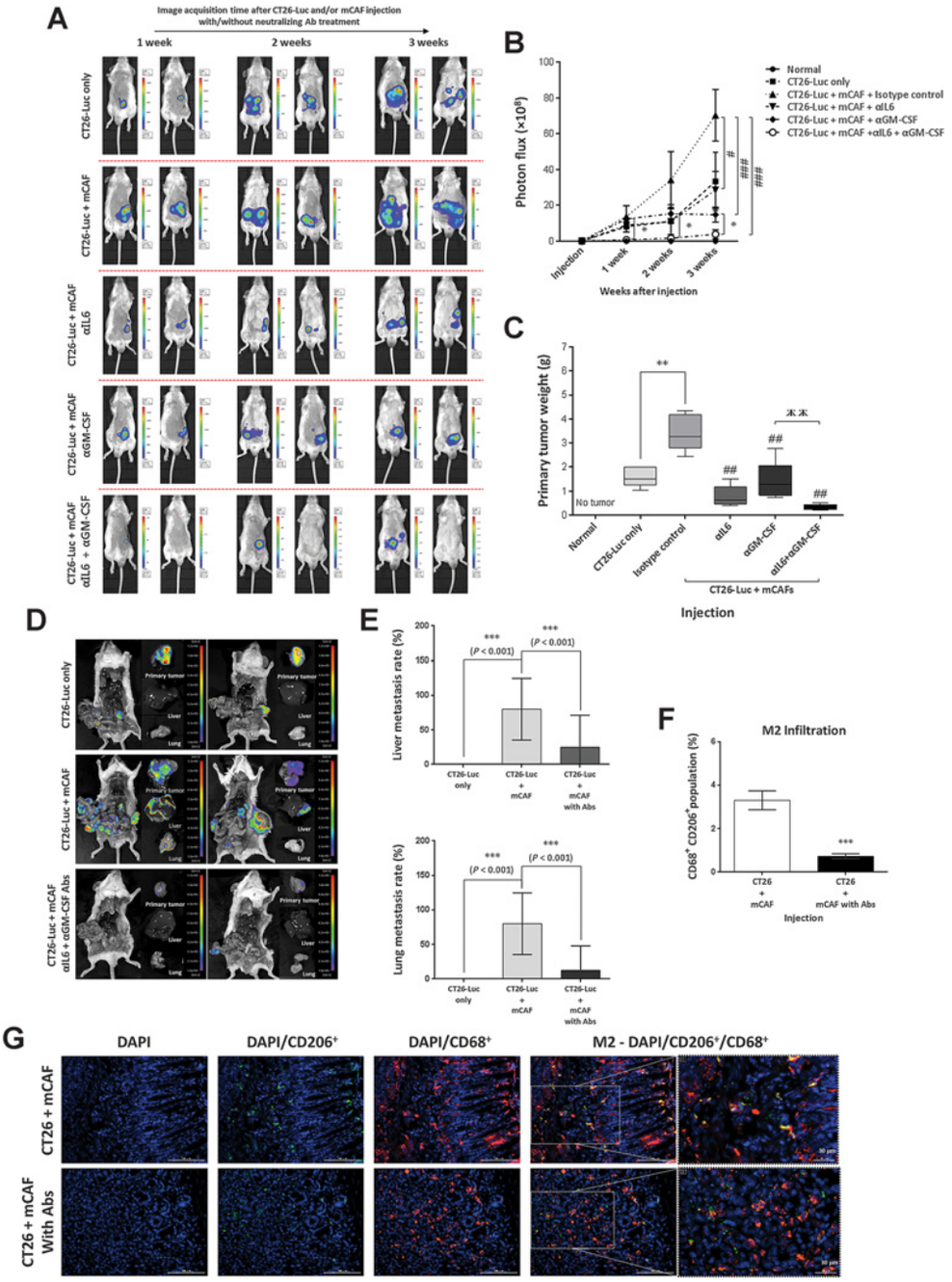

Figure 6.

IL6 and GM-CSF blockade synergistically reduce the recruitment of TAMs and inhibit metastasis. **A,** IVIS images of representative mice during the 3-week period of antibody blockade. **B,** Photon flux from cancer cells in the transplanted mice with or without antibody blockade. $n = 8$ mice/group; error, SE. **C,** Primary tumor weight in the transplanted mice. n = 8 mice/group; error, SE. **D,** IVIS images of representative dissected organs [primary tumor (upper), liver (middle) and lung (lower)] from tumor-bearing mice for metastasis. Mice were sacrificed after the 6-week period of antibody blockade. **E,** Metastasis rate for lung and liver in the transplanted mice with or without antibody blockade. $n = 10$ mice/group; error = SE. **F** and **G,** Immunohistochemical analysis of CD206 and CD68 positive cells, in the tumor tissue. The rate of double-stained cells was determined from 10 randomly selected fields of view per section and normalized for double stained cells by DAPI counter staining. The bar chart shows quantification of the merged, double-stained cells. $n = 6$; error, SE. *, $P < 0.05$; **, $P < 0.01$; ***, $P < 0.001$; #, $P < 0.05$; ##, $P < 0.01$; ###, $P < 0.001$; Ж Ж, $P < 0.01$.

monocytes or monocyte–CAF cocultures (Fig. 2A and B), suggesting that cancer cells induce CAF to secrete factors that potentiate the effects of cancer cells on monocyte differentiation. PMA is widely used to differentiate THP-1 monocytes into macrophages, which are used for subsequent differentiation into M1- or M2-type macrophages (19). Compared with PMA-treated monocytes, we show that CAFs induce THP-1 differentiation into M2-like macrophages, with increased expression of *IL10* and *TGFβ*, and reduced expression of *IL12p40* and *iNOS* (Fig. 1B). CAF stimulation with cancer cell CM increased macrophage differentiation and M2 marker expression (Fig. 2C–F). Our protocol used CM at a 1:20 dilution. This dilution should facilitate the detection of inducible factors in the CAFs, which may otherwise be "masked" by factors present in an undiluted CM.

Cytokine array analysis showed that cancer cell CM-stimulated CAFs increased the secretion of nine cytokines (Fig. 3A). Four were selected to assess their effects on monocyte differentiation and TAM recruitment: IL7, CXCL5, GM-CSF, and IL6, because they had the highest fold change of secretion. IL7 and CXCL5 had no significant effect on THP-1 monocyte differentiation (Supplementary Fig. S5). This appears to be consistent with the scientific literature. To our knowledge, there is no report linking IL7 or CXCL5 with THP-1 differentiation. The chemokine CCL7 was also upregulated in the array, but discounted from analysis because we previously reported this cytokine as a regulator of the proinvasive crosstalk in OSCC (6).

IL6 and GM-CSF induced monocyte differentiation into proinvasive macrophages (Fig. 3E; Supplementary Fig. S10). Cancer cell–mediated secretion of IL6 and GM-CSF by CAFs appears to be a feature of multiple tumor types because oral, colon, and breast carcinoma cells produced similar effects (Fig. 3D). The marker profile of macrophages differentiated by IL6 resembled an M2 type (Supplementary Figs. S7A and S8). In contrast, GM-CSF treatment increased the expression of M1 markers. However, M1 marker expression was inhibited by combined treatment with IL6. Overall, the marker profile of macrophages derived by treatment with IL6 and GM-CSF is broadly consistent with the profile observed in macrophages derived by coculture with cancer-stimulated CAFs, supporting the notion that IL6 and GM-CSF are efferent factors secreted by CAFs to promote monocyte differentiation.

BMDMs were used to assess the relevance of IL6 and GM-CSF as monocyte differentiation factors *in vivo* (Fig. 4). Flow cytometry analysis of CD11b, CD206, and CD86 expression revealed that treatment with IL6 or GM-CSF increased differentiation into $CD11b^{+}$ $CD206^{+}$ $CD86^{-}$ macrophages. Combined treatment of IL6 and GM-CSF further increased differentiation into the M2 macrophages (Fig. 4C).

The presence of M2-like TAMs is directly related to poor prognosis in colon carcinoma (23, 24). To assess the role of IL6 and GM-CSF in TAM infiltration and metastasis, we used the orthotopic, syngeneic model of colon carcinoma (Fig. 5). Recently, the benefits of this model for studying cellular interactions within developing tumors was emphasized, due to the presence of an intact immune system and nontumor cells in the ecological niche, such as vascular and stromal cells (25). The positive influence of CAFs on tumorigenesis was demonstrated by the cotransplantation of primary CAFs and colon carcinoma cells, which increased IL6 and GM-CSF levels and the infiltration of M2-like TAMs (Fig. 5G; Supplementary Figs. S14 and S15).

Our clinical data from the Oncomine database showed upregulated IL6 and GM-CSF in colon cancer, and neck/head cancer (Supplementary Table S1). Disease stage–dependent increases in IL6 or GM-CSF expression were also observed in the Bittner colon and TCGA COAD databases and the TCGA HNSC database, respectively (Supplementary Table S1). Additional clinical studies have also demonstrated increased IL6 or GM-CSF expression with disease progression. As examples, in colon cancer, IL6 expression was positively correlated with the TNM classification of malignant tumor stage (26). Increased IL6 expression was found to be associated with poor prognosis and acquired cisplatin resistance in head and neck squamous cell carcinoma (27). Serum IL6 expression was also associated with clinical parameters of colorectal cancer, such as tumor invasion, distant metastasis, and tumor stage (28). In oral squamous cell carcinoma, prevalence of the cervical lymph node or distant metastasis in the high IL6 expression group was significantly greater than the negative and low expression groups (29). For GM-CSF, an increased level of GM-CSF in serum was shown to be a potential diagnostic and prognostic marker for poor prognosis in patients with colorectal cancer (30). Enhanced GM-CSF protein levels were also found to be significantly associated with invasion and poor prognosis in patients with head/neck cancer (31).

The antibody blockade study used a dose of 100 μg antibody/mouse (Fig. 6). Assuming a mouse weight of 20 g and a human weight of 60 kg, this dose would correspond to approximately 5 mg/kg. In clinical trials, the monoclonal anti-IL6 antibody (tocilizumab) was used at a dose of 8 mg/kg for testing effects on the cardiovascular risk in patients with rheumatoid arthritis (TOCRIVAR-ClinicalTrials.gov identifier: NCT01752335). In addition, the chimeric IL6 mAb siltuximab is recommended to be used at a 11 mg/kg dose for Castleman lymphoproliferative disease (FDA approval for siltuximab: https://www.cancer.gov/about-cancer/treatment/drugs/fda-siltuximab). For GM-CSF blockade, the human monoclonal GM-CSF antibody mavrilimumab (CAM-3001) was used at a 10 mg/kg dose in patients with adult-onset rheumatoid arthritis (ClinicalTrials.gov identifier: NCT00771420) and adverse events were reported as similar between the placebo and mavrilimumab-treated groups. The human monoclonal GM-CSF antibody namilumab was used at a dose of 300 mg/patient (subcutaneous delivery), which equates to 5 mg/kg for a 60 kg patient, in a phase I trial for rheumatoid arthritis (ClinicalTrials.gov identifier: NCT01317797). Therefore, the antibody dose used for the mouse antibody blockade in Fig. 6 is broadly in line with the doses used for clinical trials. However, clinical issues may be associated with this treatment approach, including general safety concerns, such as infusion reactions/injection-site reactions, or more specific adverse effects associated with targeting cytokine networks, for example, cytokine release syndrome, or inducing immune responses against tumor cells, such as tumor lysis syndrome. These issues were also discussed in the review by Catapano and Papadopoulos (32).

CAFs can be divided into subpopulations based on their phenotype and influence in the cancer ecological niche. Waghray and colleagues recently identified a subpopulation of CAFs termed cancer-associated mesenchymal stem cells, which promote cancer invasion via GM-CSF secretion (33). Our results indicate that CAF-secreted GM-CSF promotes tumorigenesis and metastasis by inducing proinvasive TAMs. These results should be especially relevant for GM-CSF, which failed phase

III clinical trials as a cancer therapeutic (34), but is commonly used as an adjuvant for cancer vaccine development (35). Future research may focus on influence of CAF subpopulations on TAM infiltration.

IL6 is known as a protumorigenic cytokine with elevated expression in recurrent metastatic lesions compared with the primary metastasis (36). To our knowledge, unlike GM-CSF, there are relatively few publications about CAF-derived IL6 and TAM development. Our study shows for the first time that CAF-derived IL6 enhances tumor progression by promoting TAM development and infiltration. The three-way interplay of cancer cells, TAMs, and CAFs in promoting tumor progression has recently been described in prostate carcinoma and shown to be mediated by CAF-derived CXCL12 (SDF-1; ref. 37). Herein, we have discovered a new facet of this influence: CAFs integrate signals from cancer cells to activate monocyte differentiation into proinvasive TAMs, with IL6 and GM-CSF as the CAF-derived inducible factors that communicate this process.

In summary, IL6 and GM-CSF have been previously linked with monocyte activation toward the M1-type (38–41). Although GM-CSF and IL6 are widely studied cytokines, our study sheds new light on their role in developing tumors, with the first demonstration that these cytokines are the signals from cancer-activated CAFs that regulate the development of M2-like TAMs and promote metastasis. GM-CSF induces monocyte differentiation toward a M1/M2 mixed phenotype and IL6 induces monocyte differentiation toward an M2 phenotype. The flow cytometry data in Fig. 4C indicates that treatment of IL6 and GM-CSF together increases the induction of M2 markers and skewers the macrophage population toward the M2 phenotype. This reiterates the position of CAFs as "prime movers" dictating the nature of tumor-associated inflammation (Supplementary Fig. S22). These findings are supported by a recent report targeting chemerin (retinoic acid receptor responder protein 2) that reduced myeloid-derived suppressive cell infiltration and the production of IL6 and GM-CSF in hepatocellular carcinoma (42). Therefore, inducible sources of IL6 and GM-CSF are strong candidates for further assessment as regulators of proinvasive inflammation in different tumor types and patients with cancer.

Disclosure of Potential Conflicts of Interest

No potential conflicts of interest were disclosed.

Authors' Contributions

Conception and design: H. Cho, D.-W. Jung, D.R. Williams
Development of methodology: H. Cho, K.M. Loke, S.-M. Oh, J. Kim, J.-J. Min, D.-W. Jung
Acquisition of data (provided animals, acquired and managed patients, provided facilities, etc.): H. Cho, Y. Seo, K.M. Loke, S.-M. Oh, J.-H. Kim
Analysis and interpretation of data (e.g., statistical analysis, biostatistics, computational analysis): H. Cho, Y. Seo, K.M. Loke, S.-M. Oh, J. Soh, H.S. Kim, H. Lee
Writing, review, and/or revision of the manuscript: H. Cho, D.-W. Jung, D.R. Williams
Administrative, technical, or material support (i.e., reporting or organizing data, constructing databases): H. Cho, K.M. Loke, S.-W. Kim, S.-M. Oh, J. Kim, J.-J. Min
Study supervision: D.-W. Jung, D.R. Williams

Acknowledgments

D.-W. Jung and D.R. Williams are supported by a Basic Science Research Program through the NRF funded by the Korean government, MSIP (NRF-2016R1A2B4012321). This work was also supported by the GIST Research Institute (GRI) in 2018.

The costs of publication of this article were defrayed in part by the payment of page charges. This article must therefore be hereby marked *advertisement* in accordance with 18 U.S.C. Section 1734 solely to indicate this fact.

Received January 12, 2018; revised May 16, 2018; accepted June 25, 2018; published first June 29, 2018.

References

1. Masuda T, Hayashi N, Iguchi T, Ito S, Eguchi H, Mimori K. Clinical and biological significance of circulating tumor cells in cancer. Mol Oncol 2016;10:408–17.
2. Jemal A, Bray F, Center MM, Ferlay J, Ward E, Forman D. Global cancer statistics. CA Cancer J Clin 2011;61:69–90.
3. Bagley RG. The Tumor Microenvironment (Cancer Drug Discovery and Development). New York: Springer; 2010.
4. Orimo A, Gupta PB, Sgroi DC, Arenzana-Seisdedos F, Delaunay T, Naeem R, et al. Stromal fibroblasts present in invasive human breast carcinomas promote tumor growth and angiogenesis through elevated SDF-1/CXCL12 secretion. Cell 2005;121:335–48.
5. Calon A, Espinet E, Palomo-Ponce S, Tauriello DVF, Iglesias M, Céspedes MV, et al. Dependency of colorectal cancer on a TGF-beta-driven program in stromal cells for metastasis initiation. Cancer Cell 2012;22:571–84.
6. Jung DW, Che ZM, Kim J, Kim K, Kim KY, Williams D, et al. Tumor-stromal crosstalk in invasion of oral squamous cell carcinoma: a pivotal role of CCL7. Int J Cancer 2010;127:332–44.
7. Lotti F, Jarrar AM, Pai RK, Hitomi M, Lathia J, Mace A, et al. Chemotherapy activates cancer-associated fibroblasts to maintain colorectal cancer-initiating cells by IL-17A. J Exp Med 2013;210:2851–72.
8. Mantovani A, Marchesi F, Malesci A, Laghi L, Allavena P. Tumour-associated macrophages as treatment targets in oncology. Nat Rev 2017; 14:399–416.
9. Murray PJ, Wynn TA. Protective and pathogenic functions of macrophage subsets. Nat Rev 2011;11:723–37.
10. Sica A, Mantovani A. Macrophage plasticity and polarization: *in vivo* veritas. J Clin Invest 2012;122:787–95.
11. Hao NB, Lü MH, Fan YH, Cao YL, Zhang ZR, Yang SM. Macrophages in tumor microenvironments and the progression of tumors. Clin Develop Immunol 2012;2012:948098.
12. Buchsbaum RJ, Oh SY. Breast cancer-associated fibroblasts: where we are and where we need to go. Cancers 2016;8:pii:E19.
13. Kalluri R. The biology and function of fibroblasts in cancer. Nat Rev 2016;16:582–98.
14. Trouplin V, Boucherit N, Gorvel L, Conti F, Mottola G, Ghigo E. Bone marrow-derived macrophage production. J Vis Exp 2013;81: e50966.
15. Murray PJ, Allen JE, Biswas SK, Fisher EA, Gilroy DW, Goerdt S, et al. Macrophage activation and polarization: nomenclature and experimental guidelines. Immunity 2014;41:14–20.
16. Polanska UM, Acar A, Orimo A. Experimental generation of carcinoma-associated fibroblasts (CAFs) from human mammary fibroblasts. J Vis Exp 2011;56:e3201.
17. Sharon Y, Alon L, Glanz S, Servais C, Erez N. Isolation of normal and cancer-associated fibroblasts from fresh tissues by fluorescence activated cell sorting (FACS). J Vis Exp 2013;71:e4425.
18. Ding Q, Chang C-J, Xie X, Xia W, Yang J-Y, Wang S-C, et al. APOBEC3G promotes liver metastasis in an orthotopic mouse model of colorectal cancer and predicts human hepatic metastasis. J Clin Invest 2011;121: 4526–36.

19. Genin M, Clement F, Fattaccioli A, Raes M, Michiels C. M1 and M2 macrophages derived from THP-1 cells differentially modulate the response of cancer cells to etoposide. BMC Cancer 2015;15:577.
20. Mantovani A, Sica A, Sozzani S, Allavena P, Vecchi A, Locati M. The chemokine system in diverse forms of macrophage activation and polarization. Trends Immunol 2004;25:677–86.
21. Lawrence T, Natoli G. Transcriptional regulation of macrophage polarization: enabling diversity with identity. Nat Rev 2011;11:750–61.
22. Foey AD. Chapter 5: macrophages—Masters of immune activation, suppression and deviation. In: Duc GHT, editor. Immune response activation. London, United Kingdom; 2014.
23. Edin S, Wikberg ML, Dahlin AM, Rutegård J, Öberg Å, Oldenborg PA, et al. The distribution of macrophages with a M1 or M2 phenotype in relation to prognosis and the molecular characteristics of colorectal cancer. PLoS One 2012;7:e47045.
24. Zhang Y, Sime W, Juhas M, Sjolander A. Crosstalk between colon cancer cells and macrophages via inflammatory mediators and CD47 promotes tumour cell migration. Eur J Cancer 2013;49:3320–34.
25. Gould SE, Junttila MR, de Sauvage FJ. Translational value of mouse models in oncology drug development. Nat Med 2015;21:431–9.
26. Zeng J, Tang ZH, Liu S, Guo SS. Clinicopathological significance of overexpression of interleukin-6 in colorectal cancer. World J Gastroenterol 2017;23:1780–6.
27. Gao J, Zhao S, Halstensen TS. Increased interleukin-6 expression is associated with poor prognosis and acquired cisplatin resistance in head and neck squamous cell carcinoma. Oncol Rep 2016;35:3265–74.
28. Wang Z, Wu P, Wu D, Zhang Z, Hu G, Zhao S, et al. Prognostic and clinicopathological significance of serum interleukin-6 expression in colorectal cancer: a systematic review and meta-analysis. Onco Targets Ther 2015;8:3793–801.
29. Jinno T, Kawano S, Maruse Y, Matsubara R, Goto Y, Sakamoto T, et al. Increased expression of interleukin-6 predicts poor response to chemoradiotherapy and unfavorable prognosis in oral squamous cell carcinoma. Oncol Rep 2015;33:2161–8.
30. Taghipour Fard Ardekani M, Malekzadeh M, Hosseini SV, Bordbar E, Doroudchi M, Ghaderi A. Evaluation of Pre-Treatment Serum Levels of IL-7 and GM-CSF in Colorectal Cancer Patients. Int J Mol Cell Med 2014;3:27–34.
31. Montag M, Dyckhoff G, Lohr J, Helmke BM, Herrmann E, Plinkert PK, et al. Angiogenic growth factors in tissue homogenates of HNSCC: expression pattern, prognostic relevance, and interrelationships. Cancer Sci 2009;100:1210–8.
32. Catapano AL, Papadopoulos N. The safety of therapeutic monoclonal antibodies: implications for cardiovascular disease and targeting the PCSK9 pathway. Atherosclerosis 2013;228:18–28.
33. Waghray M, Yalamanchili M, Dziubinski M, Zeinali M, Erkkinen M, Yang H, et al. GM-CSF mediates mesenchymal-epithelial cross-talk in pancreatic cancer. Cancer Discov 2016;6:886–99.
34. Gupta R, Emens LA. GM-CSF-secreting vaccines for solid tumors: moving forward. Discov Med 2010;10:52–60.
35. Yu TW, Chueh HY, Tsai CC, Lin CT, Qiu JT. Novel GM-CSF-based vaccines: one small step in GM-CSF gene optimization, one giant leap for human vaccines. Human Vaccin Immunother 2016;12:3020–8.
36. Guo Y, Xu F, Lu T, Duan Z, Zhang Z. Interleukin-6 signaling pathway in targeted therapy for cancer. Cancer Treat Rev 2012;38:904–10.
37. Comito G, Giannoni E, Segura CP, Barcellos-de-Souza P, Raspollini MR, Baroni G, et al. Cancer-associated fibroblasts and M2-polarized macrophages synergize during prostate carcinoma progression. Oncogene 2014;33:2423–31.
38. Fleetwood AJ, Lawrence T, Hamilton JA, Cook AD. Granulocyte-macrophage colony-stimulating factor (CSF) and macrophage CSF-dependent macrophage phenotypes display differences in cytokine profiles and transcription factor activities: implications for CSF blockade in inflammation. J Immunol 2007;178:5245–52.
39. Fleetwood AJ, Dinh H, Cook AD, Hertzog PJ, Hamilton JA. GM-CSF- and M-CSF-dependent macrophage phenotypes display differential dependence on type I interferon signaling. J Leukoc Biol 2009;86:411–21.
40. Casella G, Garzetti L, Gatta AT, Finardi A, Maiorino C, Ruffini F, et al. IL4 induces IL6-producing M2 macrophages associated to inhibition of neuroinflammation in vitro and in vivo. J Neuroinflamm 2016;13:139.
41. Biswas SK, Mantovani A. Macrophage plasticity and interaction with lymphocyte subsets: cancer as a paradigm. Nat Immunol 2010;11:889–96.
42. Lin Y, Yang X, Liu W, Li B, Yin W, Shi Y, et al. Chemerin has a protective role in hepatocellular carcinoma by inhibiting the expression of IL-6 and GM-CSF and MDSC accumulation. Oncogene 2017;36:3599–608.